Human Molecular Genetics, 2011, Vol. 20, No. 6 **1197–1211**
doi:10.1093/hmg/ddq564
Advance Access published on January 6, 2011

Genetic mouse models for Parkinson's disease display severe pathology in glial cell mitochondria

Saskia Schmidt[1,2,*,†], Bettina Linnartz[1,2,†], Sonja Mendritzki[1,†], Teresa Sczepan[1], Matthias Lübbert[3], Christine C. Stichel[5] and Hermann Lübbert[1,2,4]

[1]Department of Animal Physiology, [2]International Graduate School of Neuroscience (IGSN) and [3]Department of Cell Physiology, Ruhr-University Bochum, 44780 Bochum, Germany, [4]Biofrontera Bioscience GmbH, 51377 Leverkusen, Germany and [5]SGO, Biology – Chemistry, 51427 Bergisch-Gladbach, Germany

Received September 13, 2010; Revised November 10, 2010; Accepted December 29, 2010

We recently described mitochondrial pathology in neurons of transgenic mice with genes associated with Parkinson's disease (PD). Now we describe severe mitochondrial damage in glial cells of the mesencephalon in mice carrying a targeted deletion of parkin (PaKO) or overexpressing doubly mutated human alpha-synuclein (asyn). The number of mitochondria with altered morphology in glial cells is cell type-dependent, but always higher than in neurons. Interestingly, mitochondrial damage also occurs in mesencephalic glia of mice carrying mutated asyn controlled by the tyrosine hydroxylase promoter. Such mice do not show glial expression of the transgene, but show expression in neighboring neurons. However, we found strong overexpression of endogenous asyn in mesencephalic astrocytes from these mice. Cortical astrocytes neither display enhanced asyn expression nor mitochondrial damage. Cultivated mesencephalic astrocytes from newborn transgenic mice display various functional defects along with the morphological damage of mitochondria. First, the mitochondrial Ca^{2+}-storage capacity is reduced in asyn transgenic mesencephalic astrocytes, but not in astrocytes from PaKO. Second, the expression of the mitochondrial protein PTEN-induced putative kinase is constitutively increased in asyn transgenic mice, while in PaKO it reacts to oxidative stress by overexpressing this protein along with other mitochondria-related proteins. Third, the neurotrophic effects exerted by control astrocytes, stimulating cortical neurons from healthy mice to develop longer processes and larger neuronal areas, are lacking in co-cultures with transgenic mesencephalic astrocytes. In summary, glial mitochondria from transgenic mice display morphological and functional alterations. Such transgenic astrocytes fail to influence neuronal differentiation, reflecting an important role that glia may play in PD pathogenesis.

INTRODUCTION

Parkinson's disease (PD) is a neurodegenerative disease characterized by the preferential, but not exclusive loss of dopaminergic neurons in the substantia nigra (SN). Most cases of PD occur sporadically at higher ages. However, 5–10% of PD cases are familial and can be attributed to mutations in genes like alpha-synuclein (asyn) or parkin (1,2). The etiology of PD remains poorly understood, but several lines of evidence imply that mitochondria play a central role in neuron death (3,4). The first indications for a direct connection between mitochondrial dysfunction and PD stem from biochemical studies at PD autopsy material, where abnormalities in the activity of respiratory chain proteins were observed (5,6). This connection was reinforced by the observation that several PD genes encode mitochondrial proteins (1). Moreover, some transgenic animals carrying PD-associated mutations develop an increased susceptibility to mitochondrial toxins (7,8), reductions in respiratory capacity (9,10) and changes in the expression of proteins related to energy metabolism (11,12). We have recently demonstrated that mouse lines overexpressing mutated human asyn (hmsyn) without or together with a parkin–Exon3 deletion exhibit an increase in the number of

*To whom correspondence should be addressed at: Department of Animal Physiology, Biology, ND5/131, Ruhr-University Bochum, 44780 Bochum, Germany. Tel: +49 2343224483; Fax: +49 2343214189; Email: saskiaschmidt@aol.com
†The authors wish to be known that, in their opinion, the first three authors should be regarded as joint First Authors.

structurally altered mitochondria in neurons (10). The structural alterations are accompanied by a reduced activity of the mitochondrial oxidative chain. Thus, the involvement of mitochondria in PD pathogenesis that has long been postulated for humans is paralleled in the transgenic and knockout mouse models.

PD is traditionally thought of as a disease of neurons. In recent years, it has nevertheless become increasingly evident that glial cells serve more than housekeeping functions. Expression of disease-linked proteins in the different glial cell (13) may lead to a disturbed physiology in these cells. In fact, several observations indicate that glial cells are active contributors to the initiation or progression of neurodegenerative diseases, additional to their obvious role in inflammation which is often interpreted as a secondary phenomenon. This is supported by cell culture data suggesting abnormal functions of glial cells with mutations in PD-associated genes (14–16).

Adding to our previous findings of severe structural and functional mitochondrial changes in neurons and the recent reports of glial involvement in neurodegenerative diseases, we now found severe morphological and functional damage in glial cell mitochondria of PD transgenic and knockout mouse models. The mouse lines used carried either a parkin–Exon3 deletion (PaKO) or overexpressed doubly mutated hmsyn, controlled by either the chicken beta-actin (BAsyn) or the mouse tyrosine hydroxylase (THsyn) promoter. It is particularly interesting that cultured mesencephalic astrocytes derived from all three genetically modified mouse lines fail to support neuronal differentiation, such as it is normally exerted by astrocytes. Taken together, our findings implicate that glial cells may be relevant or even essential contributors to the pathogenesis of PD.

RESULTS

Cellular distribution of the hmsyn in the brains of BAsyn and THsyn animals

Prior to the investigation of mitochondrial damage, we compared the distribution of the hmsyn in the transgenic asyn mouse lines. We performed sequential immunoperoxidase labeling with asyn- and cell type-specific antibodies. Both lines showed transgene expression in the brain, but the cell type expressing the transgenic proteins varied considerably between the lines. All transgene-expressing cells in the THsyn brain had a neuronal phenotype (Fig. 1A and B). The majority of these cells displayed the dopaminergic marker tyrosine hydroxylase (Fig. 1C and D). In contrast, mice of the BAsyn line showed transgene expression almost exclusively in astrocytes (Fig. 1E and F) and oligodendrocytes (investigated by electron microscopic immunohistochemistry, data not shown), while immunostaining was absent in microglia of all brain regions (data not shown).

Severe mitochondrial abnormalities in mesencephalic glial cells

Recent studies of transgenic animals reported that mutations in genes associated with familial PD induce severe destruction and functional impairments of mitochondria in neurons (10,11,17). On the other hand, it is increasingly recognized that glial cells express the PD-inducing genes (13,14,18,19). Furthermore, it is suspected that they may enhance or even induce neurodegenerative processes (12,20,21). Thus, we asked the question to which extent mitochondria from mesencephalic glial cells of PD transgenics and knockouts are also structurally affected.

Therefore, we examined the ultrastructure of glial cell mitochondria in the SN of knockout (PaKO) and transgenic (THsyn, BAsyn) mouse lines plus age-matched non-transgenic littermates (LM). In order to elucidate a potential age-dependent progression, we analyzed two different age groups of the asyn transgenic lines and three age groups of the PaKO line.

Electron microscopic analyses revealed that at all ages almost all mesencephalic glial cell types of the transgenic and knockout animals (Fig. 2D–I) exhibited a higher number of structurally altered mitochondria in glial cells compared with age-matched LM (Fig. 2A–C). These alterations comprised disintegration and reduction of mitochondrial cristae (Fig. 2E, G and I), mitochondrial enlargement and formation of protrusions or even disruption of the outer membrane (Fig. 2E). The ultrastructure of all other glial organelles appeared normal. Representative images of neurons from transgenic animals can be found in Stichel *et al.* (10).

The percentage of damaged mitochondria varied among the three different glial cell types (astrocytes, microglia and oligodendrocytes) depending on the genotype and the age of the animal.

In the PaKO line, mitochondrial damage was already noticed at 16 days and all mesencephalic glial cell types were already significantly ($P \leq 0.016$) affected at this early age (Fig. 3A, C, E). The percentage of damaged mitochondria increased during the following weeks in all glial cells (4–8-fold). Thus, in all glial cells, PaKO mice revealed damaged mitochondria at 3 months of age at a similar percentage as in older animals. In some cases, a slight reduction occurred with advancing age (Fig. 3A, C, E). At all time points, mitochondrial alterations were even higher in oligodendrocytes than in astrocytes or microglia (Fig. 3A, C, E).

In BAsyn mice, the extent of mitochondrial damage was strikingly more heterogeneous than in the other two lines. The amounts of altered mitochondria in mesencephalic astrocytes and oligodendrocytes of the THsyn and BAsyn mice were similar to those of the PaKO line (Fig. 3A and E), while microglia of BAsyn mutants revealed a substantially lower number of structural changes compared with PaKO of the same age (Fig. 3C). Similar to the PaKO line, oligodendrocytes were the most seriously affected glial cells in the asyn transgenics.

Since parkin has been reported to influence mitochondrial biogenesis (22), potentially affecting our quantitative analyses, we compared the number of all mitochondria (damaged plus healthy) in each glial cell type of the transgenic and knockout lines (Fig. 3B, D, F). The average number of mitochondria per cell type varied between the different mesencephalic glial cell types, with microglia

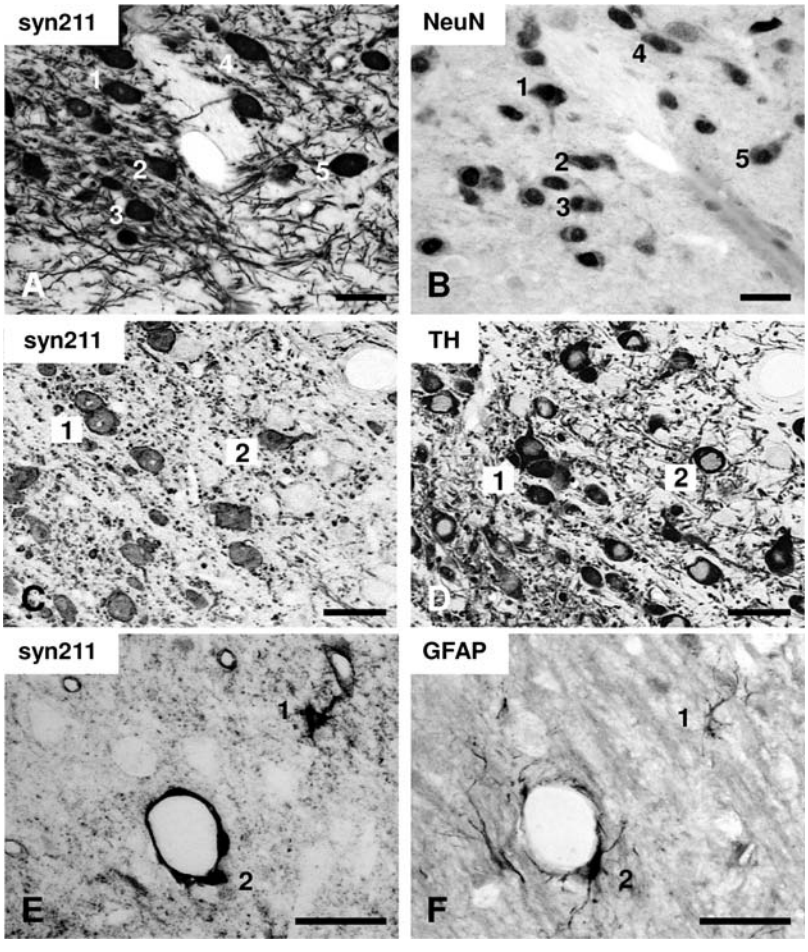

Figure 1. Light microscopic phenotyping of cells expressing the transgene in THsyn and BAsyn mouse brains. Photomicrographs of serial, 3 μm thick sections of the SN of THsyn (**A**–**D**) and BAsyn (**E** and **F**) mice. In THsyn, the syn211-immunostaining (A and C) colocalized with the markers NeuN (B) and TH (D), indicating transgene expression in catecholaminergic neurons. In BAsyn, the syn211-immunostaining (E) is found in GFAP-immunopositive astrocytes (F). Double-labeled cells are indicated by the same number. Scale bars, 30 μm.

exhibiting the lowest number (5.85 mitochondria per cell; Fig. 3D). Most importantly, we did not find differences in mean values of the total numbers of counted mitochondria between any transgenic or knockout line and the age-matched LM (Fig. 3B, D, F). To confirm this result, we re-counted the numbers of damaged or healthy mitochondria in all astrocytes of one vibratome section from SN of each of three 12–15-month-old animals from the mouse lines. Every section contained between 80 and 130 astrocytes, and the average numbers of healthy and damaged mitochondria in the mouse lines are shown in Figure 3H. Again, we did not reveal any significant differences in the numbers of mitochondria in transgenic astrocytes compared with LM.

In general, we observed that mitochondria of mesencephalic glial cells in the transgenic and knockout lines display severe structural deformations. The number of structurally altered mitochondria (i) reaches mature levels already at 3 months of age and (ii) is always highest in oligodendrocytes. The comparison of the analyzed transgenic and knockout lines reveals (iii) the largest extent of damage in PaKO glial cells and (iv) the total number of mitochondria is not changed in any glial cell type of the transgenic or knockout lines.

Comparison of glial and neuronal mitochondrial damage

In a recent publication, we reported similar mitochondrial damage in neurons of the same transgenic and knockout lines analyzed in this study (10). To address the temporal and quantitative relationship of glial and neuronal mitochondrial alterations, we completed the previous neuronal data with those of 16-day- and 3-month-old mice, reanalyzed previous neuronal data using the same statistical test as in the present study and compared the neuronal and glial data pools.

In 3-month and 12–15-month-old PaKO mice, all mesencephalic glial cells exhibited a substantially higher (2.5–7-fold) percentage of damaged mitochondria than mesencephalic neurons of the same line and age (Fig. 3A, C, E, G). The same holds true for astrocytes and oligodendrocytes of the THsyn and BAsyn lines. Hence, our comparison indicates that, in the SN of transgenic and knockout models analyzed, mitochondria in most glial cells are affected more severely than those in neurons. In addition, at the age of 3 months, mitochondrial damage in neurons was less pronounced than at higher ages, indicating a delayed development of the mitochondrial damage in neurons compared with glial cells.

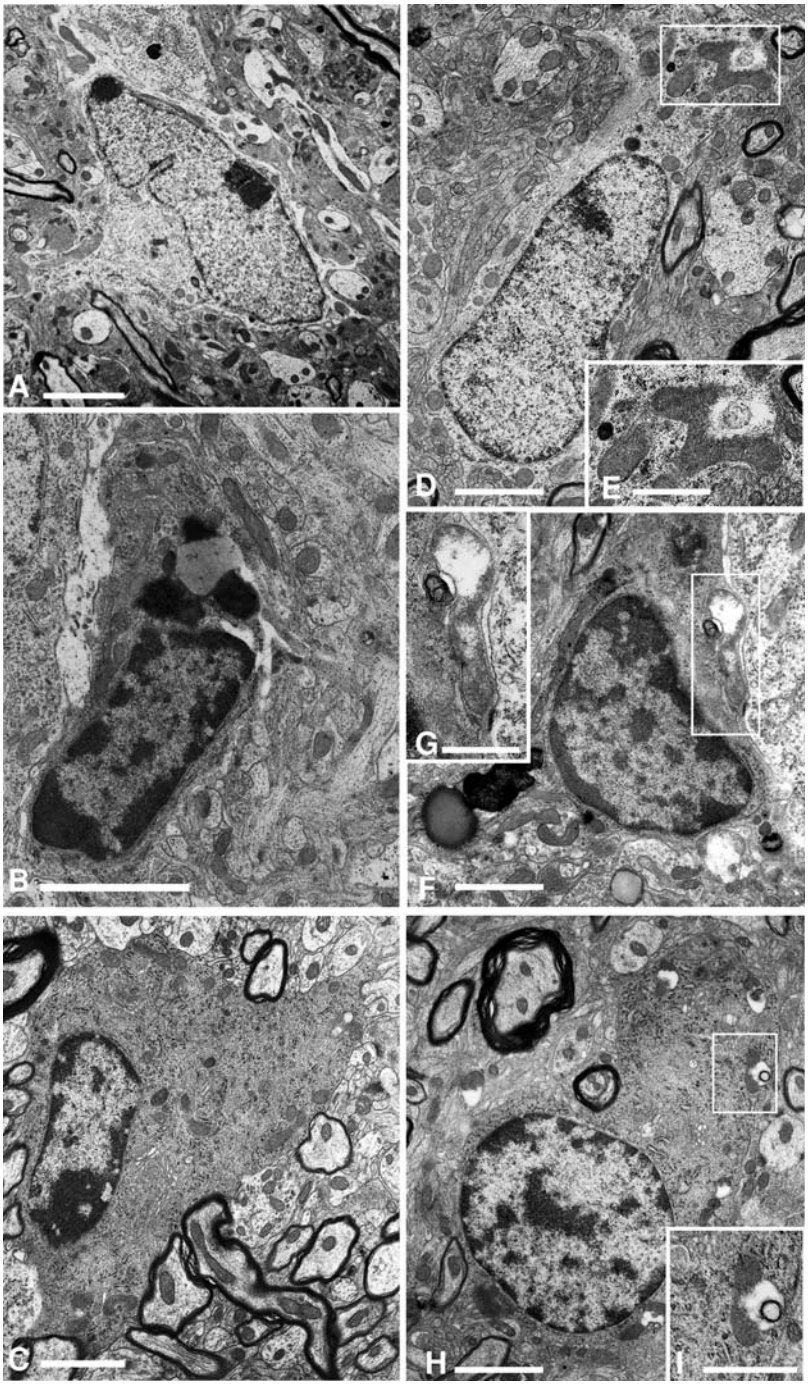

Figure 2. Structural damage of mitochondria *in situ.* Illustrations show representative examples of astrocytes (**A**, 3 months), microglial cells (**B**, 12.5 months) and oligodendrocytes (**C**, 3 months) of the SN from LM. Astrocytes of THsyn (12.5 months) are represented in (**D**), microglia and oligodendrocytes of BAsyn (3 month) in (**F**) and (**H**). Many mitochondria of transgenic mice show severe structural alterations. (**E**, **G**, **I**) Higher magnifications of boxes in the corresponding figures (D), (F) and (H). Scale bars, 2 μm (A–D, F, H) and 1 μm (E, G, I).

Transgene expression and damaged mitochondria in cultivated mesencephalic astrocytes

In order to perform functional analyses on cultured glial cells, we verified the occurrence of mitochondrial damage in cultured astrocytes from the transgenic or knockout animals. Therefore, we cultivated mesencephalic astrocytes from 1-day-old mice of the three transgenic and knockout lines. The purity of the astrocyte cultures was >86%, as determined by glial fibrillary acidic protein (GFAP) immunoreactivity.

First, we analyzed the expression of hmsyn in astrocytes of the BAsyn and THsyn mouse line by western blotting. Mesencephalic astrocytes from BAsyn displayed high levels of the transgene, while astrocytes from LM did not express hmsyn

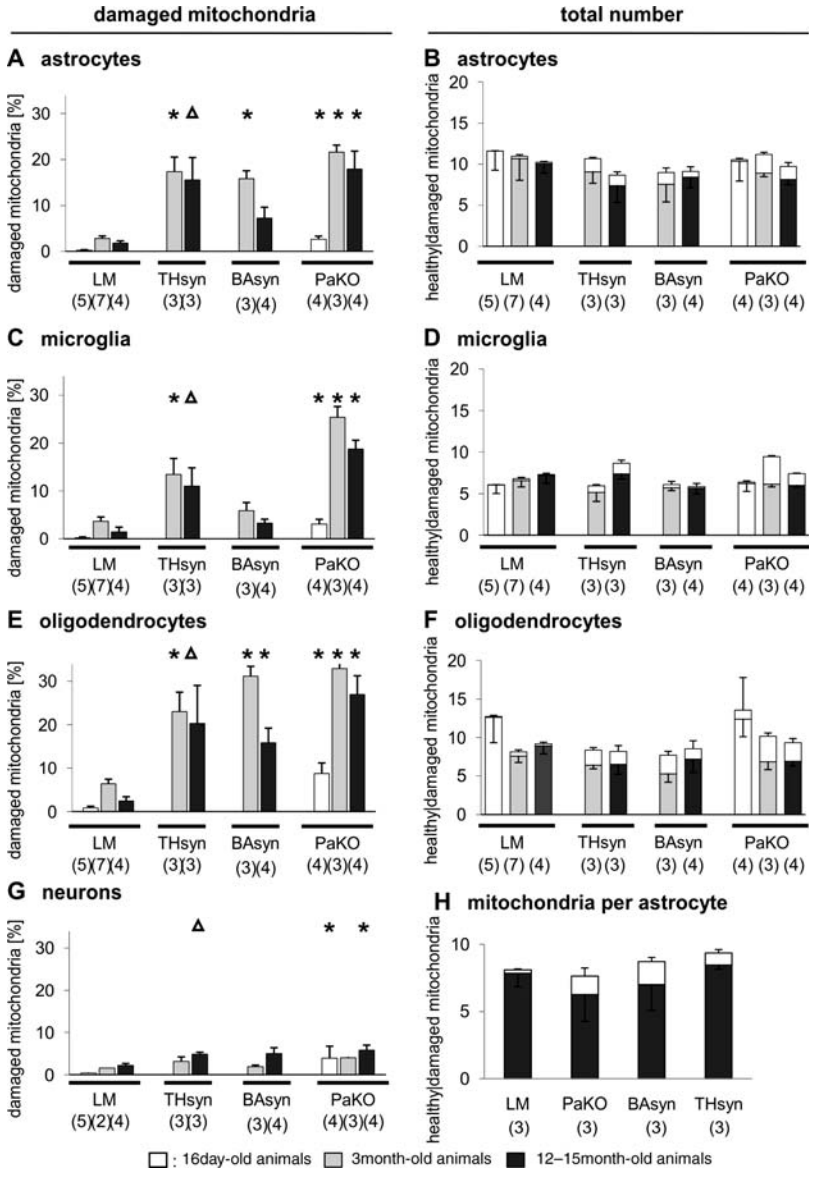

Figure 3. Quantitative analyses of structural mitochondrial changes and total number of mitochondria *in situ.* Graphs show the percentage of damaged mitochondria and the average total number of healthy (filled part of the columns) and damaged (open part of the columns) mitochondria per cell section in astrocytes (**A** and **B**), microglia (**C** and **D**), oligodendrocytes (**E** and **F**) and neurons (**G**), in the SN of THsyn, BAsyn and PaKO versus LM at 16 days, 3 months and 12–15 months of age. Compared with LM, significant increases in damaged mitochondria were found for nearly all glial cell types of the investigated transgenic and knockout lines (16 days: $^{*}P = 0.016$; 3 months: $^{*}P = 0.017$; 12–15 months: $^{*}P = 0.029$, $^{\Delta}P = 0.057$). In neurons, only the PaKO mice displayed significant damage (16 days: $^{*}P = 0.032$; 12–15 months: $^{*}P = 0.029$, $^{\Delta}P = 0.057$). The mean value of total numbers of counted mitochondria (B, D, F) varied among the different glial cell types, but there is no significant difference between the transgenic and knockout lines and the age-matched LM. Numbers in parentheses indicate numbers of analyzed animals. Error bars: $\pm$SEM. Graphs in (**H**) show the total numbers of mitochondria per astrocyte in all mesencephalic astrocytes present in vibratome sections of 12–15-month-old mice (healthy mitochondria: filled part of the columns and damaged mitochondria: open part of the columns). Error bars = SD, $n = 3$ with 80–130 cells analyzed for each mouse, one-way ANOVA.

(Fig. 4A). In contrast, astrocytes from THsyn showed no expression of the transgene (Fig. 4B). As a positive control, a lysate of the mesencephalon from THsyn was used to confirm the expression of hmsyn. However, when using an antibody recognizing both hmsyn and endogenous asyn, a strongly elevated expression of endogenous asyn was detected in mesencephalic astrocytes of THsyn astrocytes compared with LM and PaKO. A similarly elevated expression was not visible in cortical astrocytes. Although astrocytes from THsyn mice do not express hmsyn, mesencephalic, but not cortical, astrocytes express higher amounts of endogenous asyn than LM (Fig. 4B). The expression of the transgene in astrocytes of the BAsyn line and its absence in astrocytes of the THsyn line is in agreement with an earlier publication in which we published the spatial distribution of the transgene expression in these mouse lines (23).

The deletion of the parkin–exon3 causes the absence of the parkin protein in all cells of the mouse model, mimicking the

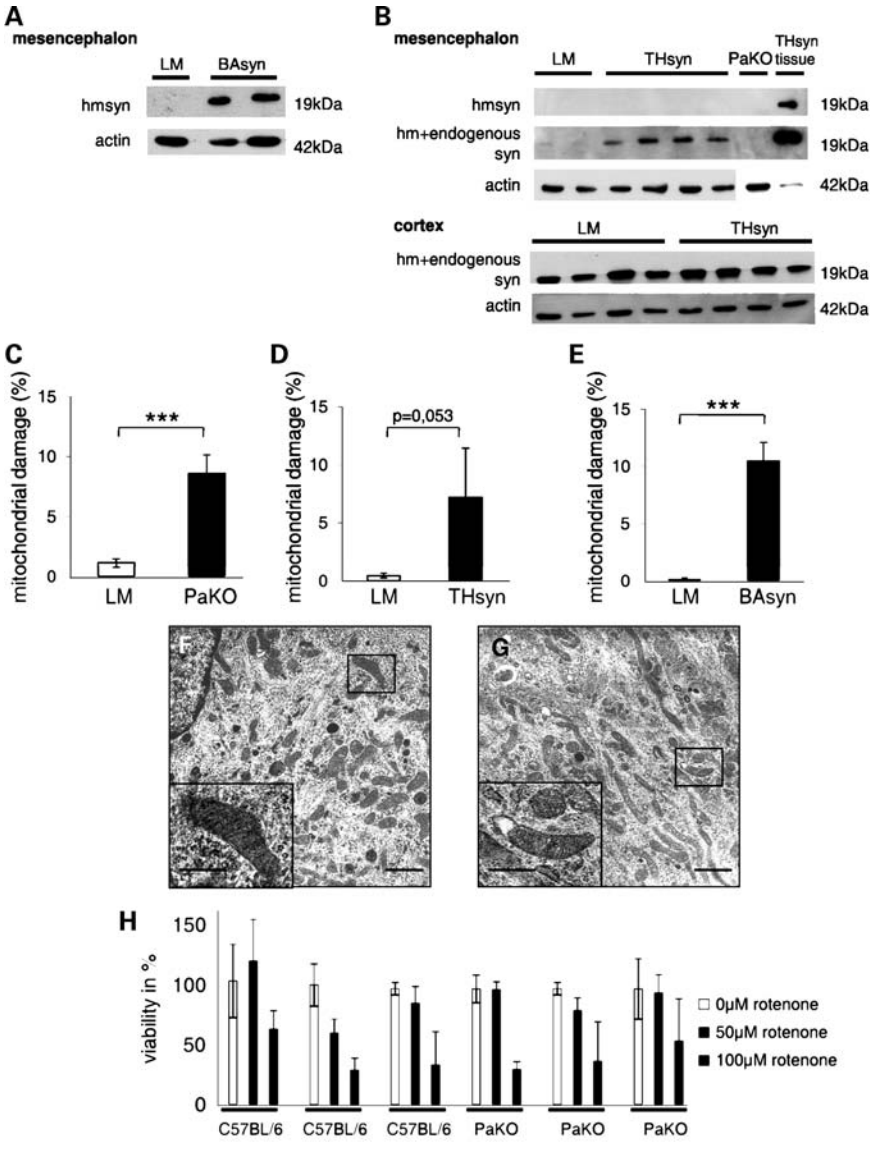

Figure 4. Structural damage of transgenic and knockout astrocytic mitochondria *in vitro* and their transgene expression. Western blots showing the expression of hmsyn of mesencephalic astrocytes from BAsyn (**A**) and of hm + endogenous asyn of mesencephalic and cortical THsyn (**B**) compared with LM. Mesencephalic brain tissue was used as positive control and PaKO astrocytes as negative control for hmsyn. Graphs show the percentage of damaged mitochondria in mesencephalic astrocytes from PaKO (**C**), THsyn (**D**) and BAsyn (**E**) compared with LM. $^{***}P < 0.001$, *t*-test, $n = 3$ independent cultures with 18 analyzed electron microscopic pictures and 600–900 counted mitochondria for each culture, error bars = SD. Representative examples of LM (**F**) and PaKO (**G**) astrocytes, scale bar = 1 μm. The higher magnifications show healthy mitochondria of LM (F) and structurally damaged mitochondria of PaKO (G), scale bar: 0.5 μm, One-way ANOVA. ATP production of C57BL/6 and PaKO astrocytes was determined after treatment with 0, 50 or 100 μM (**H**), $n = 3$, error bars = SD.

situation in the inherited human disease. To confirm the existence of parkin in non-transgenic astrocytes, we determined the parkin RNA level in mesencephalic C57BL/6J astrocytes by RT–PCR and found a strong expression that was absent in the PaKO astrocytes (data not shown).

We then asked whether the mitochondrial alterations in astrocytes described above occur already at an even earlier stage, such that they are already apparent in astrocyte cultures from 1-day-old mice. Electron microscopic analyses exhibited a substantially higher number of structurally damaged mitochondria in cultivated transgenic and knockout mesencephalic astrocytes compared with astrocytes from LM (Fig. 4C–E). Higher magnifications of mitochondria from LM and PaKO are shown in Figure 4F and G.

The percentage of damaged mitochondria was <2% in LM, but up to 10% in the knockout and transgenic mice. Already at this early age, astrocytes were highly significantly affected in PaKO (Fig. 4C) and BAsyn mice (Fig. 4E). Mitochondrial damage was clearly visible, but the variation between astrocyte cultures derived from different litters was higher in astrocytes from THsyn than those from the other two mouse lines (Fig. 4D).

This result demonstrates that morphological mitochondrial damage is already present in cultured astrocytes (14 DIV)

from newborn mice. A comparison of these results with the numbers of damaged astrocytes in 3-month-old knockout and transgenic animals showed an age-dependent increase in ultrastructural mitochondrial changes (22, 16 and 17% after 3 m in PaKO, BAsyn und THsyn mice, respectively).

We next confirmed that these mitochondrial impairments are not caused or accompanied by an increased cell death rate, which we determined by the lactate dehydrogenase activity neither with or without stress induction by H_2O_2. We neither observed an increased degeneration of the cultivated cells nor an elevated susceptibility to oxidative stress (data not shown). In addition, we tested the susceptibility of astrocytes from PaKO to rotenone, an inhibitor of the mitochondrial respiratory chain. Mesencephalic astrocytes from C57BL/6 or PaKO displayed no difference in their sensitivities to different concentrations of rotenone (Fig. 4H). Moreover, to determine whether the astrocytes are functional in energy production, we measured the resting membrane potential of transgenic and LM astrocytes by Patch Clamp recordings and did not find any significant differences (LM: -62.8 ± 8.6 mV; BAsyn: -61.1 ± 12.8 mV).

Reduced astrocytic mitochondrial Ca^{2+}-storage capacity

Since our results indicate changes in mitochondrial morphology, we asked the question whether these impairments are accompanied by changes in mitochondrial function. Mitochondria, next to the endoplasmic reticulum (ER), serve as Ca^{2+} stores of the cell. Therefore, we analyzed the mitochondrial Ca^{2+}-storage capacity by applying the fluorescent dye fura-2 AM. This dye gets excited at the wavelengths of 340 nm (Ca^{2+}-bound) or 380 nm (Ca^{2+}-unbound). Through this ability, fura-2 AM is frequently used to determine altered levels of Ca^{2+} in the cytosol. We exposed the cells in intervals of 2 s to 1 ms light pulses, alternating at 340 or 380 nm, to detect Ca^{2+} release from internal stores by changes in the ratio of the two wave lengths. An ATP stimulus (10^{-4} M, 10 s) was first applied to release Ca^{2+} from internal stores. Ca^{2+} is subsequently removed from the cytosol by mitochondria (24) and was then depleted by a 10 s stimulus with carbonyl cyanide 4-(trifluoromethoxy)phenylhydrazone (FCCP; 10^{-5} M), an uncoupler of the mitochondrial electron transport chain. Afterwards, the cells were again stimulated with ATP to control the integrity of the Ca^{2+} response. Examples for results from LM mesencephalic astrocytes are shown in Figure 5A, D and G. In comparison, both asyn transgenics displayed a decreased FCCP peak, illustrating a reduced mitochondrial Ca^{2+}-storage capacity (THsyn: Fig. 5E, BAsyn: Fig. 5H). Calculating the mean values of the maximal ATP and FCCP peaks from four to seven different experiments revealed a statistically significant reduction in mitochondrial Ca^{2+} release after FCCP treatment for THsyn (Fig. 5F) and BAsyn (Fig. 5I) astrocytes. In contrast, mesencephalic astrocytes from PaKO did not display a similar decrease in mitochondrial Ca^{2+} storage (Fig. 5B and C).

Upregulation of mitochondria-related proteins in transgenic and knockout astrocytes

Alterations in mitochondrial ultrastructure and mitochondrial calcium storage capacity might be accompanied by changes in the expression of proteins related to mitochondria. We compared the expression of the proteins PTEN-induced putative kinase 1 (PINK1), dynamin like protein-1 (Drp1), superoxide dismutase 2 (SOD2), mortalin and cytochrome c with and without stress induction by H_2O_2. We calculated the protein content in percent of actin for the single blots (Fig. 6B, E, H) and the ratios between protein levels after H_2O_2 treatment and protein levels without treatment. Cultivated mesencephalic astrocytes from PaKO show a statistically significant upregulation of the proteins PINK1 (Fig. 6D–F), Drp1 (Fig. 6A–C) and SOD2 (Fig. 6G–I) upon oxidative stress that is absent in astrocytes from non-transgenic littermates (Fig. 6C, F, I). We did not detect a similar upregulation of the proteins after stress induction in both asyn transgenic lines (data not shown). However, in these animals, we found PINK1 more abundantly expressed even without stimulation by H_2O_2. In contrast, Drp1, SOD2, mortalin and cytochrome c showed no differential expression with or without stress induction (data not shown). Representative blots for PINK1 expression in THsyn astrocytes are shown in Figure 6J and in BAsyn astrocytes in Figure 6L. Western blots were repeated at least three times. The graph in Figure 6K represents the quantification of the THsyn and the graph in Figure 6M that of the BAsyn blot.

Effects of transgenic and knockout mesencephalic astrocytes on neuronal differentiation

To analyze whether the functionally and morphologically impaired astrocytes exhibit a disturbed interaction with neurons, knockout, transgenic and non-transgenic mesencephalic astrocytes were co-cultured with non-transgenic cortical C57BL/6J neurons derived from 15-day-old embryos. The experimental setup chosen was such that astrocytes were seeded in culture well inserts and cultivated in the same medium with neurons without direct contact for 2 days. Immunostaining with cell-type-specific antibodies revealed that the neuronal cultures contained >95% neurons. The shape and complexity of the neurons were described by the following parameters: (i) length of the longest process and (ii) total neuronal area (area covered by neuritic arbor). A characteristic example of a neuron co-cultured with LM astrocytes, as depicted in Figure 7A, displayed long processes, quite different from a neuron that was co-cultured with BAsyn astrocytes (Fig. 7B). The latter exhibited substantially shorter processes. Neurons co-cultured with astrocytes from LM developed longer processes as well as larger neuron areas compared with neurons cultivated without astrocytes (Fig. 7C–H). Neurons also exhibited highly significantly shorter processes when co-cultured with either PaKO, THsyn or BAsyn astrocytes, similar to neurons in control experiments in which the inserts did not contain astrocytes (Fig. 7C, E, G). Furthermore, the presence of astrocytes from the transgenic or knockout mouse lines led to smaller total neuronal areas (Fig. 7D, F, H). The differences were statistically significant for THsyn and BAsyn and displayed a strong tendency for PaKO.

In summary, neurons co-cultured with transgenic, knockout or without astrocytes show similar growth. Analysis of both parameters revealed that transgenic and knockout mesencephalic astrocytes have little or no positive effect on neuronal

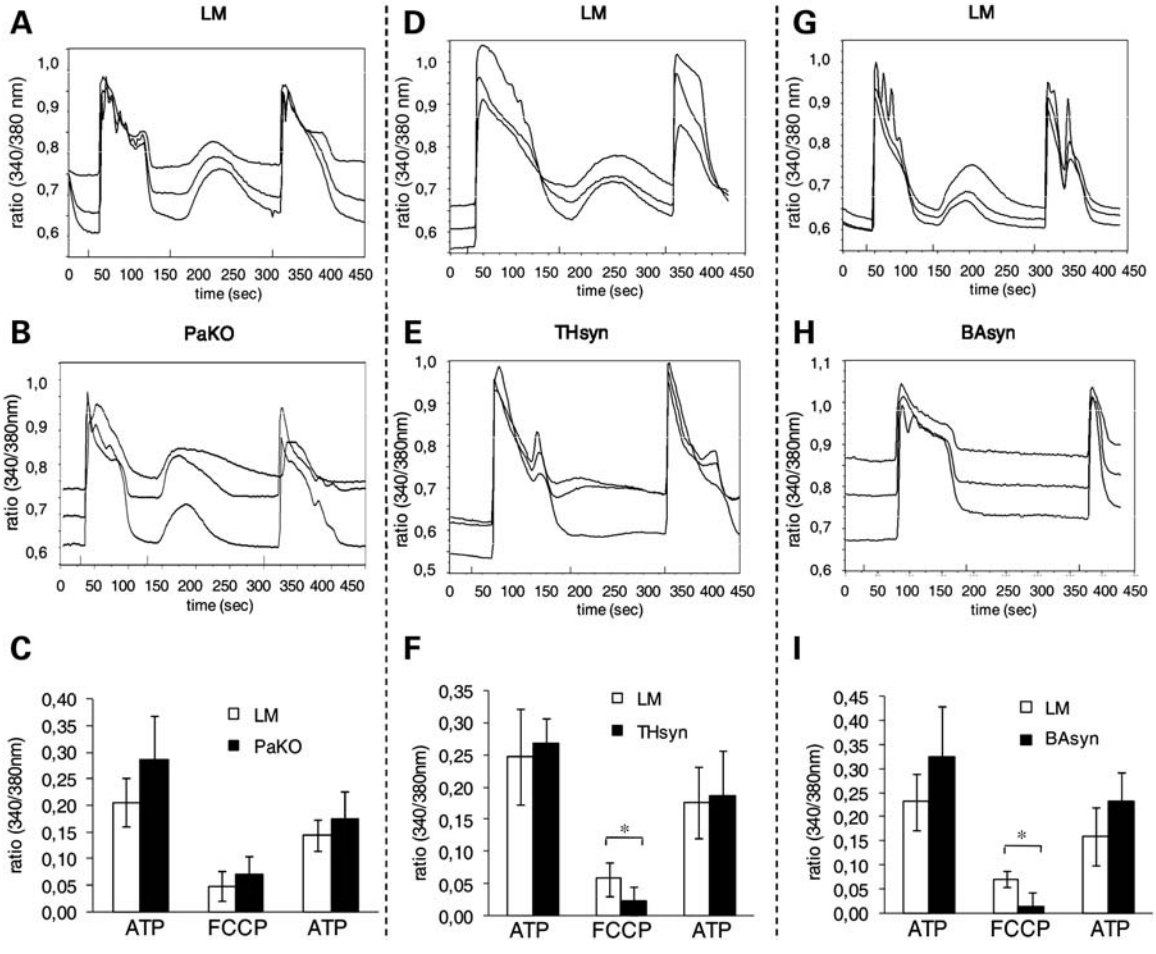

Figure 5. Mitochondrial Ca^{2+} release from astrocytes. Ca^{2+} release from intracellular stores was determined after ATP or FCCP stimulus. Representative curves are shown for LM (**A**, **D**, **G**), PaKO (**B**), THsyn (**E**) and BAsyn (**H**). ATP was added first, and then FCCP was injected after return of the ratio to the baseline, followed after 180 s by a second application of ATP. Mean values of the maximum curve peak (normalized to baseline) are calculated for PaKO (**C**), THsyn (**F**) and BAsyn (**I**) compared with LM. Error bars = SD, $n = 4–7$ independent cultures with two to eight cells each, $^*P < 0.05$, *t*-test.

morphology. This is strikingly different from the effects seen in co-cultures with LM astrocytes and indicates a functional disturbance of neuron–glia interactions. Moreover, we could show that the transfer of astrocyte-conditioned media had the same effects on the neuronal differentiation (data not shown).

These results implicate that the impaired support to neurons provided by the transgenic astrocytes is caused either by the lack of a soluble supportive factor or by the existence of a soluble toxic factor. To distinguish these two possibilities, we serially diluted medium conditioned with LM astrocytes either with (i) medium conditioned with PaKO astrocytes (Fig. 8A and B) or (ii) with unconditioned medium (Fig. 8C and D). The effects of the serial dilutions were expected to be very similar in case of a lack of a supportive factor, and different if a toxic factor was secreted by the transgenic or knockout astrocytes. For serial dilutions (i) and (ii), a sequential decrease in the trophic support was observed, down to the level of the PaKO-conditioned or -unconditioned media. It is unlikely that a secreted toxic factor would show a similar distribution and, thus, it was postulated that the knockout or transgenic mesencephalic astrocytes lack the production of a trophic factor.

Obvious candidates for the trophic factors might be brain-derived neurotrophic factor (BDNF) or glial cell line-derived neurotrophic factor (GDNF). To test whether they are responsible for the effects observed, we supplemented our co-culture system with BDNF or GDNF. Neither of the two neurotrophic factors enhanced the neuronal differentiation parameters when neurons were co-cultured with transgenic astrocytes (shown for BAsyn in Fig. 9A–D).

DISCUSSION

The most prominent feature of PD pathogenesis is the degeneration of dopaminergic neurons. The degenerative process involves structural and functional mitochondrial dysfunctions (25,26) and the accumulation of reactive oxygen species (27). Our latest studies on mouse models overexpressing doubly mutated hmsyn or exhibiting the loss of parkin revealed structural impairments of mitochondria in neurons (10).

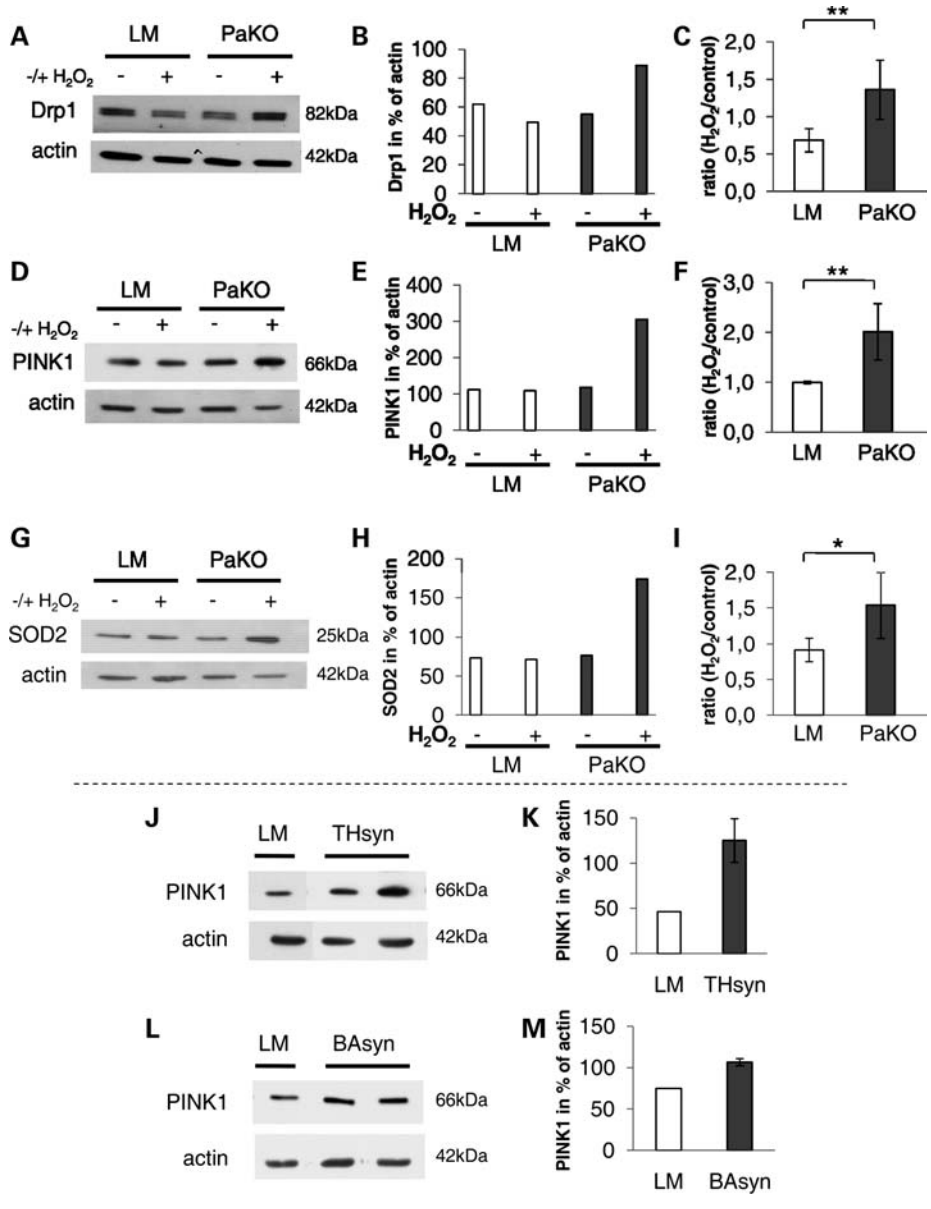

Figure 6. Response of transgenic and knockout astrocytes to oxidative stress. Representative western blots are shown for the expression of Drp1 (**A**), PINK1 (**D**) and SOD2 (**G**) in PaKO astrocytes. The densitometric analyses of the single blots (**B**, **E**, **H**) and mean values of the ratios (H_2O_2/control) of three to six cultures (**C**, **F**, **I**) are shown for the three proteins. Representative western blots and densitometric analyses of PINK1 expression in THsyn (**J**, **K**) and BAsyn (**L**, **M**) astrocytes compared with LM are shown in (J–M). Equal amounts of protein were loaded and expression of actin was used as loading control. Error bars = SD, three to five independent blots each.

In this work, we demonstrate that these mouse models show severe ultrastructural mitochondrial alterations also in the different mesencephalic glial cell types. The extent of mitochondrial damage in glial cells is always higher than that in neurons and, unlike the damage in neurons, has reached maximal levels already at an age of 3 months. Interestingly, our data implicate that, at least in asyn transgenic mice, the expression of the transgene in a glial cell is not a necessary requirement for the presence of damaged mitochondria in the same cell. Instead, we found an overexpression of the endogenous asyn that occurred in mesencephalic, but not cortical, astrocytes and may be causing the mitochondrial changes.

Mitochondrial damage in mesencephalic glial cells was in some cases slightly lower in 12–15-month-old PD transgenics and knockouts than in the corresponding 3-month-old mice. To the contrary, in neurons we found the highest levels of damaged mitochondria in the oldest animals. In mammalian cells, mitochondria are degraded by autophagy (28), which seems to preferentially remove damaged mitochondria (29). Through this mechanism, impaired mitochondria may be removed and then replaced by healthy ones. The lower numbers of altered glial mitochondria in 12–15-month-old mice may reflect the activity of this mechanism. If this was the reason, one would have to assume that mitochondrial

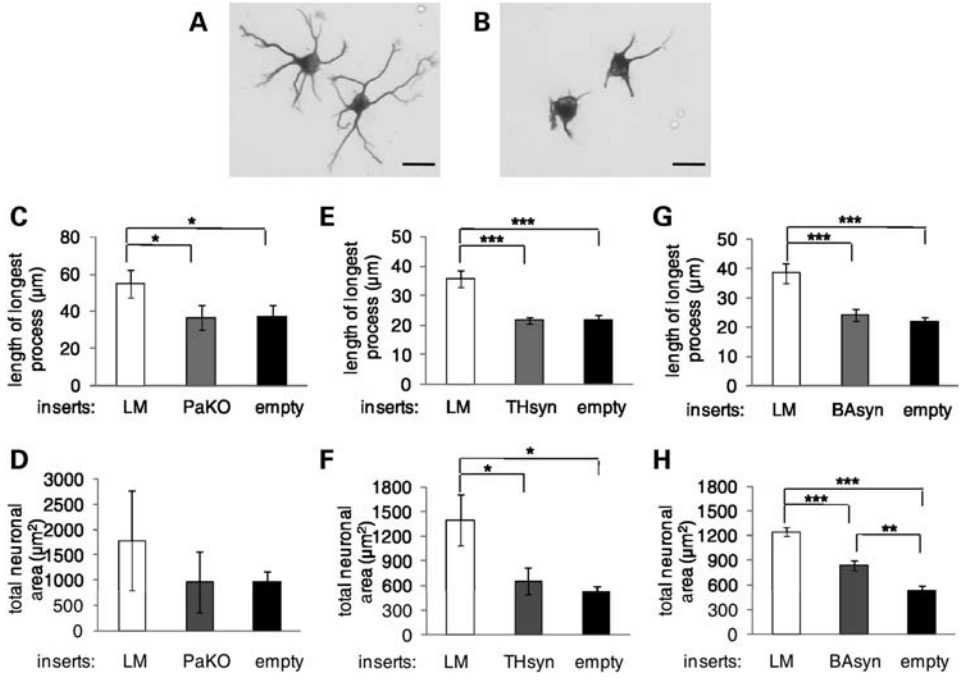

Figure 7. Influence of transgenic and knockout astrocytes on neuronal differentiation. Examples of neurons co-cultured with LM (**A**) or BAsyn (**B**) astrocytes, scale bar = 20 µm. The length of the longest process was measured for neurons co-cultured with LM, knockout/transgenic [PaKO (**C**), THsyn (**E**), BAsyn (**G**)] or without astrocytes. The quantified total neuronal area is shown in (**D**), (**F**) and (**H**). Error bars = SD, $n = 3$, $^{*}P < 0.05$, $^{**}P < 0.01$, $^{***}P < 0.001$, one-way ANOVA.

damage occurs less frequently in glial cells from older animals, such that the damaged mitochondria can gradually be replaced.

It is known that Parkin contributes to mitochondrial degradation (30). Therefore, we also analyzed the total number of mitochondria per astrocyte in the SN from the transgenic and knockout mouse lines. However, we did not find any differences in the numbers of mitochondria. These results indicate that there are either no changes in the autophagy of mitochondria or that there is an increased autophagy which cannot be detected due to a decreased rate of mitochondrial fission. In *Drosophlia*, it has been shown that parkin null mutants show defects in mitochondrial fission (31).

Furthermore, we demonstrate that structural mitochondrial damage occurs already in mesencephalic astrocytes derived from 1-day-old mice carrying these PD-inducing mutations and maintained in culture for 14 days. Mitochondrial alterations were more consistently found in PaKO and BAsyn compared with THsyn. In the latter line, the variability between different experiments was higher, possibly suggesting that the damage occurred at variable extents at this young age of the animals. It is particularly interesting that glial cells from THsyn do not express the mutant protein, but express higher amounts of the endogenous asyn compared with LM. It may be considered whether this is related to the integration site of the transgene. The integration site of our BAsyn mouse line is in the gene RP24-323B22.1 on Chr. 4-A3 while that of the THsyn is unknown. Another explanation for the high expression of endogenous asyn in mesencephalic THsyn glial cells might be an early interaction between neurons (which express the transgene) and glial cells. The possible basis of this interaction could be the mutated asyn itself. Several studies have shown that asyn is secreted by neurons (32–34). The protein could be taken up by glial cells (35–37) and cause a persistent enhancement of the endogenous asyn expression. The high expression of the endogenous asyn seems likely to cause the pathophysiological effects observed in THsyn astrocytes. This hypothesis is strengthened by the fact that cortical astrocytes of THsyn do not express higher amounts of the endogenous asyn. It is known from other animal models that overexpression of non-mutated asyn leads to asyn-immunopositive inclusion bodies (38) and an increased density of dopamine transporter as well as an enhanced toxicity to the neurotoxin 1-methyl-4-phenyl-1,2,3,6-tetrahydropyridine (8).

In this context, it is interesting to note that we did not find mitochondrial damage or any of the altered mitochondrial functions in cortical astrocytes from THsyn mice (data not shown), indicating that the close vicinity to neurons expressing the transgene in the mesencephalon is indeed required to induce the upregulation of the endogenous asyn.

Even though the latter explanation for the enhanced expression of endogenous asyn in mesencephalic astrocytes is more complicated than a pure integration effect, the difference between mesencephalic and cortical astrocytes renders this possibility more likely.

In further experiments, we investigated functional impairments caused by the morphological alterations of mitochondria. In our earlier work describing mitochondrial deficits in neurons, we found a reduced complex I activity of the respiratory chain in parkin knockout animals. Since our technology does not allow to determine complex I activity in the small cell

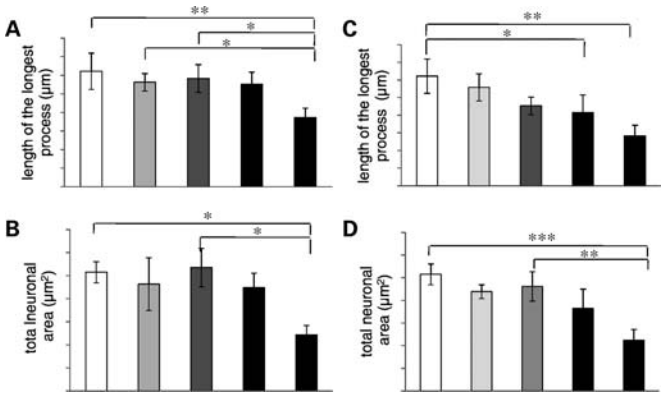

Figure 8. Medium transfer after serial dilution of conditioned media. Neuronal differentiation was measured after growing of neurons in serial dilutions of astrocyte conditioned medium from LM and PaKO. The length of the longest process is shown in (**A**) and total neuronal area in (**B**). Serial dilutions of astrocyte conditioned medium from LM with unconditioned medium are shown in (**C**) (length of the longest process) and (**D**) (total neuronal area). Error bars = SD, $n = 3$, $^{*}P < 0.05$, $^{**}P < 0.01$, $^{***}P < 0.001$, one-way ANOVA.

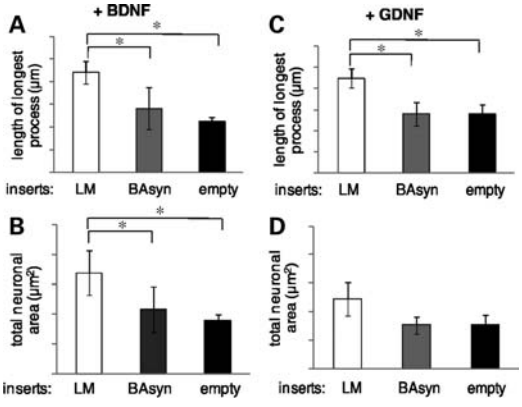

Figure 9. Influence of transgenic astrocytes on neuronal differentiation with neurotrophic factor. The length of the longest process was measured for neurons co-cultured with LM, BAsyn or without astrocytes ± BDNF or ± GDNF (**A** and **C**). The quantified total neuronal area is shown in (**B**) and (**D**). Error bars = SD, $n = 3$, $^{*}P < 0.05$, one-way ANOVA.

numbers in astrocytes cultures, we have here concentrated on other mitochondrial functions. The ER and mitochondria are the main intracellular Ca^{2+} stores, albeit the ER has a 10^4 times higher storage capacity than mitochondria. However, Ca^{2+} released from the ER is rapidly removed from the cytosol by transport into mitochondria (24). Mitochondrial Ca^{2+} stores furthermore play an important role in the physiology of the cell since mitochondrial Ca^{2+} uptake increases ATP production. ATP in turn is required for ER Ca^{2+} cycling (39). To determine whether the mitochondrial Ca^{2+}-storage capacity is altered in astrocytes from our transgenic and knockout mice, we applied FCCP as an uncoupler of the mitochondrial electron transport chain. We found a statistically significant decrease in Ca^{2+} release from astrocytic mitochondria of both asyn transgenic mouse lines. Treatment of astrocyte cultures with ATP revealed a higher amount of total Ca^{2+} released in PaKO, BAsyn and THsyn cells. A potentially related observation has previously been described for cells transfected with human doubly mutated asyn, which had a higher plasma membrane ion permeability (40,41). Most interestingly, similar to the foregoing we saw this effect also in THsyn astrocytes which themselves lack the expression of the transgene but stem from the vicinity of neurons expressing the mutated asyn.

Both parkin and asyn seem to be involved in the maintenance of mitochondrial integrity. We could show that the altered mitochondrial structure is associated with an increased expression of mitochondria-related proteins. In PaKO astrocytes, the proteins PINK1, Drp1 and SOD2 are upregulated upon stress induction with ROS. In contrast, astrocytes from both asyn transgenics displayed a higher expression of PINK1 already under normal conditions, but did not show similar reactions to ROS treatment. Since asyn is metabolized by parkin (4), its overexpression may partly mimic the effects of the parkin knockout. Both PINK1 and Drp1 are involved in the mitochondrial fission and fusion machinery (31,42,43). PINK1 acts in the same pathway with parkin (42) and mutations in PINK1 are also known to cause PD (44). Therefore, upregulation of these proteins might be related to the observed mitochondrial alterations. An increased expression of SOD2 hints towards an over-active stress response, characterized by a stronger degradation of superoxides. In summary, mitochondria-related proteins are differentially regulated due to mutations inducing PD. Since an aberrant regulation of expression of PINK1 is detected in all three transgenic and knockout mouse lines and the PINK1 gene is related to PD itself, PINK1 may play a prominent role in the disease processes induced by parkin or asyn.

In spite of the morphological and functional mitochondrial changes in all glial cell types, we did not find any evidence for an insufficient energy production in these cells. Cell survival under normal conditions or oxidative stress, membrane potential and the sensitivity to rotenone are all unchanged. A subcritical reduction in energy production may be the explanation for the lack of neuronal degeneration in these animal models (10).

As mesencephalic astrocytes from all transgenic and knockout mouse lines display ultrastructural and functional mitochondrial impairments, we concluded that the metabolism of the entire cell may be disturbed. Therefore, we investigated the influence of these cells on the differentiation of wild-type neurons. Neurons co-cultured in the same medium with LM astrocytes developed longer processes and covered larger areas than without the astrocyte co-culture. However, mesencephalic astrocytes from PaKO, THsyn and BAsyn were not able to support neuronal growth. Neurons cultured together with these astrocytes looked similar to those cultured in the absence of astrocytes. The experimental setup using inserts with astrocytes does not allow a direct physical contact between the astrocytes and the neurons. It is not yet known if and how the lack of trophic support provided by the astrocytes is related to the altered mitochondrial features seen in this study. The fact that astrocytes from THsyn mice, which lack expression of the transgene but show an enhanced expression of endogenous asyn, apparently cause the same effects on neuronal differentiation as astrocytes from PaKO and BAsyn, strengthens the hypothesis that adjacent transgene

expressing neurons are able to exert a lasting influence on astrocyte physiology.

The results suggest that astrocytes from all three transgenic and knockout mouse lines exhibit a defective release of soluble factors supporting neuronal differentiation (45) or release factors which are toxic to the neurons. The dilution experiments indicated that the lacking support of transgenic and knockout astrocytes to neuronal differentiation are due to the lack of neurotrophic factors. Culturing neurons in media consisting of dilutions of the LM medium with the PaKO medium resulted in a better neuronal outgrowth than a dilution of the LM medium with unconditioned medium. It seems that PaKO-conditioned media contain also amounts of neurotrophic factors leading to a better neuronal outgrowth in the different dilutions with the LM medium than the dilutions of LM with unconditioned medium.

GDNF and BDNF are secreted by astrocytes and influence the differentiation of neurons. Previous studies show a positive effect of these factors on the survival and differentiation of both TH-positive (46) and cortical neurons (47,48). Therefore, we added GDNF and BDNF to our co-culture system; however, adding one of these two neurotrophic factors does not rescue the failure in the neuronal differentiation. These results lead to the assumption that maybe other soluble factors are absent or that a combination of many neurotrophic factors is needed for a normal neuronal outgrowth.

Regardless of whether mice exhibit the loss of parkin or overexpress human doubly mutated asyn, mesencephalic glial cells from all transgenic and knockout mouse lines displayed severe and early structural mitochondrial changes. Functional deficits of astrocytes differed between the various transgenic and knockout lines. Astrocytes from PaKO showed an unusual upregulation of PINK1, Drp1 and SOD2 upon stress induction, which was lacking in cells from both asyn lines. The latter two lines instead exhibited a stronger expression of PINK1 already under normal conditions, but did not react to ROS treatment in the same way as PaKO astrocytes. Furthermore, they displayed a reduced Ca^{2+}-storage capacity which was not seen in the PaKO cells. In spite of these differences, we demonstrated that astrocytes isolated from all three transgenic and knockout mouse lines isolated at P1 and maintained in culture for 14 days have mitochondrial deficits and lack the trophic support for neurons provided by control astrocytes. While astrocytes from THsyn did generally not express the transgene, mesencephalic astrocytes from these mice displayed an increased expression of endogenous asyn. Overexpression of endogenous asyn apparently caused similar effects as the doubly mutated hmsyn expressed in astrocytes from BAsyn. This indicates that the overexpression of asyn *per se* triggers the observed effects. It remains to be shown though, if and how the expression of the transgene in neighboring neurons in the mesencephalon triggers an overexpression of the endogenous asyn that is stable over 10 DIV in culture. Even though we do not yet have a full understanding of the interactions of mutated PD proteins and their influence on the functional parameters described here, our results provide further support to the assumption that glial cells contribute to the early pathogenesis of PD.

MATERIALS AND METHODS

Transgenic and knockout mouse lines

Three different transgenic and knockout mouse lines were analyzed in this study: (i) a homozygous parkin-deficient line with a targeted deletion of exon3 (PaKO) which was backcrossed with wild-type C57BL/6J for three generations (F4-generation; 94% C57BL/6J and 6% 129SvJ) and two asyn transgenic lines (C57BL/6J background) carrying the doubly mutated (A30P and A53T) hmsyn, driven by either (ii) the chicken beta-actin promoter (BAsyn) or (iii) the mouse tyrosine hydroxylase promoter (THsyn). Control mice were age-matched non-transgenic littermates (LM). The generation, behavioral and histopathological analyses of these lines have already been described (10,23,49).

Housing and breeding of the animals were performed in accordance with the German guidelines of the animal care and use committee. All efforts were made to minimize the number of animals used and their suffering.

In situ

Tissue preparation. Mice were anesthetized with an overdose of ketamine (100 mg/kg) and rompun (5 mg/kg) and perfused transcardially with phosphate-buffered saline (PBS), followed by 4% paraformaldehyde (PFA) in 0.1 M phosphate buffer (PB) for immunohistochemistry or 2% PFA plus 2.5% glutaraldehyde (GA) in PB for electron microscopy. Brains were immediately removed and postfixed.

Immunohistochemistry. For sequential double-labeling brains were embedded in paraffin. Serial sagittal 3 μm thick sections were deparaffinized and antigen retrieval (5–10 min cooking in 0.01 M citrate buffer, pH 6.0) was performed (except for GFAP). After preincubation (3% normal serum), adjacent sections were treated with mouse anti-hmsyn (anti-syn211; 1:700, Invitrogen, Karlsruhe, Germany), astrocyte marker rabbit anti-cow GFAP (anti-GFAP; 1:250; Acris, Hiddenhausen, Germany), neuronal marker mouse anti-mouse NeuN (anti-NeuN; 1:700; Chemicon, Schwalbach, Germany), microglia marker goat anti-human ionized calcium-binding adaptor molecule 1 (anti-ionized calcium-binding adaptor molecule 1; 1:1000; Abcam, Cambridge, UK) or sheep anti-rat tyrosine hydroxylase as marker for catecholaminergic neurons (anti-TH; 1:500; Millipore, Schwalbach, Germany). Sections were treated by the corresponding biotinylated secondary antibody (1:300, Axxora, Lörrach, Germany), ABC reagent (1:100; Axxora) and silver-gold intensification (50).

Transmission electron microscopy. Postfixed (2 h, 4°C) brains were cut with a vibratome (100 μm thick), the SN samples microdissected and placed in 2% OsO_4 for 1 h. Samples were then dehydrated with graded concentrations of ethanol and Epon-propylene oxide and flat embedded in Epon. Representative ultrathin sections were collected on Formvar-coated grids and contrasted with uranyl acetate and lead citrate.

Data analysis. Peroxide-labeled immunostained samples were visualized at the microscopic level (Axioskop 2, Zeiss) under brightfield illumination. Images were captured with an

imaging system (JVC, KYF75U camera) connected to a computer equipped with an image program (Diskus 4.50, Hilgers).

Ultrathin sections were visualized using a Phillips EM-410 or Zeiss EM 900. Morphology and number of mitochondria were evaluated in digitized electron microscopic images of 16 days, 2–3 months and 12–15 months old animals. In total, 18–24 somata per cell type taken from two vibratome sections of each animal were independently analyzed by two examiners blind with respect to genotype and age of mice. Following numbers of animals were analyzed:

(i) *LM* [16 days: $n = 5$, 2–3months: $n = 7$ (glial cells), $n = 2$ (neurons); 12–15 months: $n = 4$],
(ii) *PaKO* (16 days: $n = 4$, 2–3 months: $n = 3$; 12–15 months: $n = 4$),
(iii) *THsyn* (2–3 months: $n = 3$; 12–15 months: $n = 3$),
(iv) *BAsyn* (2–3 months: $n = 3$; 12–15 months: $n = 4$).

To elucidate the numbers of mitochondria per astrocyte, we counted all astrocytes on whole microdissected samples of 12–15-month-old mice ($n = 3$) with 80–130 cells each.

Ultrathin sections were selected at random from the middle of vibratome sections to avoid potential structural irregularities possibly occurring on the surface.

Glial cells were counted if they contained a nucleus surrounded by cytoplasm and were classified according to their typical ultrastructural features (51,52). Briefly, astrocytes were identified by their electron-lucent cytoplasm and the appearance of their nuclei (thin rim of heterochromatin adjacent to nuclear membrane). Microglia display usually an oval or elongated nucleus with prominent clumps of chromatin throughout the nucleoplasm. Their cytoplasm contains quite commonly lysosomes and lipofuscins. Oligodendrocytes show electron-dense cytoplasms and their nuclei are rich in clumped heterochromatin close to the border of the nucleus.

Mitochondria were classified as structurally damaged when one or more of the following alterations were observed: distorted or disrupted cristae, detachment of or protrusions from the outer membrane, electron-lucent domains or inclusions in the matrix (Fig. 2). Data are presented as a mean $\pm$ SD of the means of the analyzed animals per genotype.

Statistical analyses of ultrastructural changes compared with corresponding age-matched LMs were carried out using Mann–Whitney rank-sum test (*U*-test, two-tailed, alpha level 0.05). The same test was used to verify statistical significances among the age groups of one genotype and the same age groups of the different genotypes (SigmaStat3.5).

Cell culture

Primary mesencephalic astrocyte cultures. Astrocytes were prepared from the mesencephalon of PaKO, transgenic THsyn and BAsyn newborn pups and the corresponding LM. After removing the meninges, the mesencephalon was dissected, diced into small fragments and incubated in 0.04 mg DNaseI and 0.1% trypsin at 37°C for 15 min. Following centrifugation, the pellets were resuspended with fire-polished glass pipettes in trituration solution containing 0.5 mg/ml trypsin inhibitor, 0.002 mg/ml DNaseI and 1 mg/ml BSA. Cell suspensions were again centrifugated and the pellets resuspended in culture medium [DMEM (*Dulbecco's modified Eagle Medium*) with GlutaMAX™ (Invitrogen), 10% normal horse serum, 100 U/ml penicillin, 100 μg/ml streptomycin and 2.5 μg/ml fungizone] and seeded on poly-D-lysine (Sigma-Aldrich, Munich, Germany) coated cell culture flasks. For our analyses, we pooled the mesencephalons of two animals of the same genotype. Culture media were refreshed twice per week. After 14 days, cultures were seeded for experiments.

Primary cortical neuron cultures. Dissociated primary neurons were prepared from the cerebral cortex of 15-day-old C57BL/6J embryos. Meninges were removed and tissue was incubated with 0.1% trypsin and 0.04 mg DNase for 30 min. The DMEM medium with 10% normal horse serum was added and cells were centrifuged for 2 min at 900 rpm. After trituration with a fire-polished glass pipette, cells were seeded at a density of 1×10^5 cells/ml on cover slips in the neurobasal medium supplemented with 1 mM L-glutamine and B-27 supplement (Invitrogen).

Indirect co-culturing and medium transfer. To analyze the effect of astrocytes on the neuronal differentiation, we performed indirect co-cultures with wild-type cortical neurons and transgenic or knockout astrocytes (transwell co-culture system; 0.4 μm pore size; BD Biosciences, Heidelberg, Germany) or we transferred astrocyte-conditioned medium to neurons. Neurons were allowed to adhere for 2 h to poly-D-lysine and laminin-coated cover slips (Invitrogen). Subsequently, transwell inserts with the confluent astrocytic cell layers were added or we removed the half of the culture media and added astrocyte-conditioned media. After 2 days in indirect co-culture neurons or a medium transfer, neurons were analyzed by immunohistochemistry and morphometrics. To test the effect of BDNF (Invitrogen) and GDNF (Invitrogen) on the co-cultures, we added 10 μg/ml of the neurotrophic factors to the co-cultures.

Immunocytochemical characterization. Immunohistochemical staining was used to characterize the composition of astrocyte and neuron cultures and to identify neurons for morphometric analyses in the indirect co-culture conditions. Therefore, cells were fixed with 4% PFA, preincubated with 5% serum plus 0.1% Triton and incubated with primary antibodies [GFAP for astrocytes (1:1000, Acris) and beta-III-tubulin (1:1000, Sigma-Aldrich) for neurons]. Primary antibody binding was visualized using the corresponding biotinylated secondary antibody, ABC reagent and a silver-gold intensification (50).

Morphometric analyses. Morphometric analyses of neurons were performed after 2 days *in vitro* (DIV), using the computer program ImageJ. Sixty beta-III-tubulin-immunopositive neurons chosen at random from three different cover slips (~20 neurons/cover slip) were analyzed for each co-culture condition and experiment. Results are expressed as mean values of three independent experiments each.

Transmission electron microscopy of cells in culture. For EM analyses, cells were seeded on aclar film (Plano, Wetzlar, Germany) in a 24-well plate for 4 days. Then astrocytes

were fixed with 2.5% GA in 0.1 M PB for 60 min and placed in 2% OsO_4 for an additional hour. After dehydration with graded concentrations of ethanol and Epon-propylene oxide, cells were embedded in Epon. Ultrathin sections were collected on Formvar-coated grids and contrasted with uranyl acetate and lead citrate. Three independent cultures of each genotype with 18 astrocytic somata each were counted.

Viability assay. Astrocytes were exposed to different concentrations of the environmental chemical rotenone (Sigma-Aldrich) dissolved in 10% dimethyl sulfoxide. ATP production was measured 24 h after treatment via CellTiter-Glo® Luminescent Cell Viability Assay (Promega, Mannheim, Germany).

Western blotting. Protein expression in astrocytes was analyzed by western blotting as described previously (10). The following primary antibodies were used: mouse anti-rat Drp1 (1:1000, BD Biosciences); mouse anti-pigeon cytochrome c (1:1.000, BD Pharmingen, Heidelberg, Germany); goat anti-human GRP75 (mortalin; 1:10.000, Santa Cruz Biotechnology, Heidelberg, Germany); rabbit anti-human PINK1 (1:10.000, Santa Cruz Biotechnology); rabbit anti-human SOD2 (1:200.000, Abcam); mouse anti-hmsyn (syn211; 1:1000, Invitrogen); and rabbit anti hmsyn (hm + endogenous asyn; 1:100, Santa Cruz Biotechnology). Western blot signals were quantified using the image analysis software TINA 2.09 and normalized against the endogenous actin level.

Cellular fluorescence measurements. Intracellular Ca^{2+} was measured with the Ca^{2+}-sensitive fluorescent dye fura-2 AM (Invitrogen). Cells were washed with extracellular recording solution containing: 145 mM NaCl, 5 mM KCl, 2 mM $CaCl_2$, 1 mM $MgCl_2$, 10 mM HEPES, pH 7.3. Then the cells were incubated for 45 min with 5 μM fura-2 AM and 0.02% pluronic (Invitrogen) before the cover slips were placed in a recording chamber. Measurements were performed under an inverted epifluorescence microscope using a high-speed polychromator system and a Xenon lamp and images were collected by a sensitive CCD camera. The MetaFluor software was used for data evaluation and illustration. For analysis of mitochondrial Ca^{2+} storage with fura-2 AM, four to seven independent cell cultures for each genotype with two to eight cells each were imaged.

Patch clamp. Patch clamp recordings were performed at room temperature using an EPC7 amplifier, an ITC-18 interface and the Pulse software (HEKA, Lambrecht, Germany). Patch pipettes were pulled from borosilicate glass (1.17 × 1.50 × 100 mm, Science Products, Hofheim, Germany) and were fire polished to a 3–5 MΩ tip resistance using a horizontal pipette puller (Zeitz Instruments, Munich, Germany). The extracellular solution used for electrophysiological recordings contained 140 mM NaCl, 5 mM KCl, 2 mM $CaCl_2$, 1 mM $MgCl_2$ and 10 mM HEPES; pH 7.3. The patch pipette was filled with 140 mM KCl, 1 mM $MgCl_2$, 0.13 mM $CaCl_2$, 1 mM EGTA, 10 mM HEPES, 2 mM ATP; pH 7.3. For LM, a total of 20 cells from four animals and for BAsyn a total of 21 cells from six animals were measured.

Statistical analyses. Data are presented as the mean ± SD of the means of the analyzed animals per genotype. Statistical analyses were performed using the Student's *t*-test or one-way ANOVA. Statistical significance was assumed at $P < 0.05$ (SigmaStat3.5).

ACKNOWLEDGEMENTS

The authors thank Petra Jergolla, Katja Schmidtke, Renate Scholl, Katrin Schuster, Holger Schlierenkamp and Silvia Schweer for excellent technical assistance.

Conflict of Interest statement. None declared.

FUNDING

This work was supported by the German National Academic Foundation (S.M.), the International Graduate School of Neuroscience Bochum (B.L., S.S.), the Research School of the Ruhr-University Bochum (B.L., S.M., S.S.) and Biofrontera Bioscience GmbH.

REFERENCES

1. Biskup, S., Gerlach, M., Kupsch, A., Reichmann, H., Riederer, P., Vieregge, P., Wullner, U. and Gasser, T. (2008) Genes associated with Parkinson syndrome. *J Neurol.*, **255**(Suppl. 5), 8–17.
2. Schiesling, C., Kieper, N., Seidel, K. and Kruger, R. (2008) Review: familial Parkinson's disease—genetics, clinical phenotype and neuropathology in relation to the common sporadic form of the disease. *Neuropathol. Appl. Neurobiol.*, **34**, 255–271.
3. Abou-Sleiman, P.M., Muqit, M.M. and Wood, N.W. (2006) Expanding insights of mitochondrial dysfunction in Parkinson's disease. *Nat. Rev. Neurosci.*, **7**, 207–219.
4. Schapira, A.H. (2008) Mitochondria in the aetiology and pathogenesis of Parkinson's disease. *Lancet Neurol.*, **7**, 97–109.
5. Mizuno, Y., Ohta, S., Tanaka, M., Takamiya, S., Suzuki, K., Sato, T., Oya, H., Ozawa, T. and Kagawa, Y. (1989) Deficiencies in complex I subunits of the respiratory chain in Parkinson's disease. *Biochem. Biophys. Res. Commun.*, **163**, 1450–1455.
6. Schapira, A.H.V., Cooper, J.M., Dexter, D., Jenner, P., Clark, J.B. and Marsden, C.D. (1989) Mitochondrial complex I deficiency in parkinsons-disease. *Lancet*, **1**, 1269.
7. Song, D.D., Shults, C.W., Sisk, A., Rockenstein, E. and Masliah, E. (2004) Enhanced substantia nigra mitochondrial pathology in human alpha-synuclein transgenic mice after treatment with MPTP. *Exp. Neurol.*, **186**, 158–172.
8. Richfield, E.K., Thiruchelvam, M.J., Cory-Slechta, D.A., Wuertzer, C., Gainetdinov, R.R., Caron, M.G., Di Monte, D.A. and Federoff, H.J. (2002) Behavioral and neurochemical effects of wild-type and mutated human alpha-synuclein in transgenic mice. *Exp. Neurol.*, **175**, 35–48.
9. Palacino, J.J., Sagi, D., Goldberg, M.S., Krauss, S., Motz, C., Wacker, M., Klose, J. and Shen, J. (2004) Mitochondrial dysfunction and oxidative damage in parkin-deficient mice. *J. Biol. Chem.*, **279**, 18614–18622.
10. Stichel, C.C., Zhu, X.R., Bader, V., Linnartz, B., Schmidt, S. and Lubbert, H. (2007) Mono- and double-mutant mouse models of Parkinson's disease display severe mitochondrial damage. *Hum. Mol. Genet.*, **16**, 2377–2393.
11. Periquet, M., Corti, O., Jacquier, S. and Brice, A. (2005) Proteomic analysis of parkin knockout mice: alterations in energy metabolism, protein handling and synaptic function. *J. Neurochem.*, **95**, 1259–1276.
12. Poon, H.F., Frasier, M., Shreve, N., Calabrese, V., Wolozin, B. and Butterfield, D.A. (2005) Mitochondrial associated metabolic proteins are selectively oxidized in A30P alpha-synuclein transgenic mice—a model of familial Parkinson's disease. *Neurobiol. Dis.*, **18**, 492–498.
13. Mori, F., Tanji, K., Yoshimoto, M., Takahashi, H. and Wakabayashi, K. (2002) Demonstration of alpha-synuclein immunoreactivity in neuronal

and glial cytoplasm in normal human brain tissue using proteinase K and formic acid pretreatment. *Exp. Neurol.*, **176**, 98–104.
14. Austin, S.A., Floden, A.M., Murphy, E.J. and Combs, C.K. (2006) Alpha-synuclein expression modulates microglial activation phenotype. *J. Neurosci.*, **26**, 10558–10563.
15. Solano, R.M., Casarejos, M.J., Menendez-Cuervo, J., Rodriguez-Navarro, J.A., Garcia, d.Y. and Mena, M.A. (2008) Glial dysfunction in parkin null mice: effects of aging. *J. Neurosci.*, **28**, 598–611.
16. Mullett, S.J. and Hinkle, D.A. (2009) DJ-1 knock-down in astrocytes impairs astrocyte-mediated neuroprotection against rotenone. *Neurobiol. Dis.*, **33**, 28–36.
17. Martin, L.J., Pan, Y., Price, A.C., Sterling, W., Copeland, N.G., Jenkins, N.A., Price, D.L. and Lee, M.K. (2006) Parkinson's disease alpha-synuclein transgenic mice develop neuronal mitochondrial degeneration and cell death. *J. Neurosci.*, **26**, 41–50.
18. Stichel, C.C., Augustin, M., Kuhn, K., Zhu, X.R., Engels, P., Ullmer, C. and Lubbert, H. (2000) Parkin expression in the adult mouse brain. *Eur. J. Neurosci.*, **12**, 4181–4194.
19. Huang, Y., Song, Y.J., Murphy, K., Holton, J.L., Lashley, T., Revesz, T., Gai, W.P. and Halliday, G.M. (2008) LRRK2 and parkin immunoreactivity in multiple system atrophy inclusions. *Acta Neuropathol.*, **116**, 639–646.
20. Croisier, E. and Graeber, M.B. (2006) Glial degeneration and reactive gliosis in alpha-synucleinopathies: the emerging concept of primary gliodegeneration. *Acta Neuropathol.*, **112**, 517–530.
21. Lobsiger, C.S. and Cleveland, D.W. (2007) Glial cells as intrinsic components of non-cell-autonomous neurodegenerative disease. *Nat. Neurosci.*, **10**, 1355–1360.
22. Kuroda, Y., Mitsui, T., Kunishige, M., Shono, M., Akaike, M., Azuma, H. and Matsumoto, T. (2006) Parkin enhances mitochondrial biogenesis in proliferating cells. *Hum. Mol. Genet.*, **15**, 883–895.
23. Maskri, L., Zhu, X., Fritzen, S., Kuhn, K., Ullmer, C., Engels, P., Andriske, M., Stichel, C.C. and Lubbert, H. (2004) Influence of different promoters on the expression pattern of mutated human alpha-synuclein in transgenic mice. *Neurodegener. Dis.*, **1**, 255–265.
24. Jouaville, L.S., Ichas, F. and Mazat, J.P. (1998) Modulation of cell calcium signals by mitochondria. *Mol. Cell. Biochem.*, **184**, 371–376.
25. Hayashida, K., Oyanagi, S., Mizutani, Y. and Yokochi, M. (1993) An early cytoplasmic change before Lewy body maturation: an ultrastructural study of the substantia nigra from an autopsy case of juvenile parkinsonism. *Acta Neuropathol. (Berl.)*, **85**, 445–448.
26. Keeney, P.M., Xie, J., Capaldi, R.A. and Bennett, J.P. Jr (2006) Parkinson's disease brain mitochondrial complex I has oxidatively damaged subunits and is functionally impaired and misassembled. *J. Neurosci.*, **26**, 5256–5264.
27. Henchcliffe, C. and Beal, M.F. (2008) Mitochondrial biology and oxidative stress in Parkinson disease pathogenesis. *Nat. Clin. Pract. Neurol.*, **4**, 600–609.
28. Terman, A., Gustafsson, B. and Brunk, U.T. (2007) Autophagy, organelles and ageing. *J. Pathol.*, **211**, 134–143.
29. Elmore, S.P., Qian, T., Grissom, S.F. and Lemasters, J.J. (2001) The mitochondrial permeability transition initiates autophagy in rat hepatocytes. *FASEB J.*, **15**, 2286–2287.
30. Geisler, S., Holmstrom, K.M., Skujat, D., Fiesel, F.C., Rothfuss, O.C., Kahle, P.J. and Springer, W. (2010) PINK1/Parkin-mediated mitophagy is dependent on VDAC1 and p62/SQSTM1. *Nat. Cell Biol.*, **12**, 119–131.
31. Deng, H., Dodson, M.W., Huang, H. and Guo, M. (2008) The Parkinson's disease genes pink1 and parkin promote mitochondrial fission and/or inhibit fusion in Drosophila. *Proc. Natl Acad. Sci. USA*, **105**, 14503–14508.
32. Sung, J.Y., Park, S.M., Lee, C.H., Um, J.W., Lee, H.J., Kim, J., Oh, Y.J., Lee, S.T., Paik, S.R. and Chung, K.C. (2005) Proteolytic cleavage of extracellular secreted alpha-synuclein via matrix metalloproteinases. *J. Biol. Chem.*, **280**, 25216–25224.
33. Fortin, D.L., Nemani, V.M., Voglmaier, S.M., Anthony, M.D., Ryan, T.A. and Edwards, R.H. (2005) Neural activity controls the synaptic accumulation of alpha-synuclein. *J. Neurosci.*, **25**, 10913–10921.
34. Lee, S.J. (2008) Origins and effects of extracellular alpha-synuclein: implications in Parkinson's disease. *J. Mol. Neurosci.*, **34**, 17–22.
35. Zhang, W., Wang, T., Pei, Z., Miller, D.S., Wu, X., Block, M.L., Wilson, B., Zhang, W., Zhou, Y., Hong, J.S. *et al.* (2005) Aggregated alpha-synuclein activates microglia: a process leading to disease progression in Parkinson's disease. *FASEB J.*, **19**, 533–542.
36. Cahoy, J.D., Emery, B., Kaushal, A., Foo, L.C., Zamanian, J.L., Christopherson, K.S., Xing, Y., Lubischer, J.L., Krieg, P.A., Krupenko, S.A. *et al.* (2008) A transcriptome database for astrocytes, neurons, and oligodendrocytes: a new resource for understanding brain development and function. *J. Neurosci.*, **28**, 264–278.
37. Chew, S.H. (2004) Phagocytosis of degenerating myelin in transected feline optic nerve: an immunohistochemical study. *Biotech. Histochem.*, **79**, 177–183.
38. Lo, B.C., Ridet, J.L., Schneider, B.L., Deglon, N. and Aebischer, P. (2002) alpha-Synucleinopathy and selective dopaminergic neuron loss in a rat lentiviral-based model of Parkinson's disease. *Proc. Natl Acad. Sci. USA*, **99**, 10813–10818.
39. Szabadkai, G. and Duchen, M.R. (2008) Mitochondria: the hub of cellular Ca2+ signaling. *Physiology (Bethesda)*, **23**, 84–94.
40. Furukawa, K., Matsuzaki-Kobayashi, M., Hasegawa, T., Kikuchi, A., Sugeno, N., Itoyama, Y., Wang, Y., Yao, P.J., Bushlin, I. and Takeda, A. (2006) Plasma membrane ion permeability induced by mutant alpha-synuclein contributes to the degeneration of neural cells. *J. Neurochem.*, **97**, 1071–1077.
41. Marongiu, R., Spencer, B., Crews, L., Adame, A., Patrick, C., Trejo, M., Dallapiccola, B., Valente, E.M. and Masliah, E. (2009) Mutant Pink1 induces mitochondrial dysfunction in a neuronal cell model of Parkinson's disease by disturbing calcium flux. *J. Neurochem.*, **108**, 1561–1574.
42. Clark, I.E., Dodson, M.W., Jiang, C., Cao, J.H., Huh, J.R., Seol, J.H., Yoo, S.J., Hay, B.A. and Guo, M. (2006) Drosophila pink1 is required for mitochondrial function and interacts genetically with parkin. *Nature*, **441**, 1162–1166.
43. Poole, A.C., Thomas, R.E., Andrews, L.A., McBride, H.M., Whitworth, A.J. and Pallanck, L.J. (2008) The PINK1/Parkin pathway regulates mitochondrial morphology. *Proc. Natl Acad. Sci. USA*, **105**, 1638–1643.
44. Valente, E.M., Abou-Sleiman, P.M., Caputo, V., Muqit, M.M., Harvey, K., Gispert, S., Ali, Z., Del Turco, D., Bentivoglio, A.R., Healy, D.G. *et al.* (2004) Hereditary early-onset Parkinson's disease caused by mutations in PINK1. *Science*, **304**, 1158–1160.
45. Mena, M.A., de Bernardo, S., Casarejos, M.J., Canals, S. and Rodriguez-Martin, E. (2002) The role of astroglia on the survival of dopamine neurons. *Mol. Neurobiol.*, **25**, 245–263.
46. Meyer, M., Matarredona, E.R., Seiler, R.W., Zimmer, J. and Widmer, H.R. (2001) Additive effect of glial cell line-derived neurotrophic factor and neurotrophin-4/5 on rat fetal nigral explant cultures. *Neuroscience*, **108**, 273–284.
47. Pozas, E. and Ibanez, C.F. (2005) GDNF and GFRalpha1 promote differentiation and tangential migration of cortical GABAergic neurons. *Neuron*, **45**, 701–713.
48. Ohgoh, M., Kimura, M., Ogura, H., Katayama, K. and Nishizawa, Y. (1998) Apoptotic cell death of cultured cerebral cortical neurons induced by withdrawal of astroglial trophic support. *Exp. Neurol.*, **149**, 51–63.
49. Zhu, X.R., Maskri, L., Herold, C., Bader, V., Stichel, C.C., Gunturkun, O. and Lubbert, H. (2007) Non-motor behavioural impairments in parkin-deficient mice. *Eur. J. Neurosci.*, **26**, 1902–1911.
50. Stichel, C.C., Singer, W. and Zilles, K. (1990) Ultrastructure of PkC(II/III)-immunopositive structures in rat primary visual cortex. *Exp. Brain Res.*, **82**, 575–584.
51. Liu, H.M. and Bahu, R.M. (1975) Ultrastructure of the nervous system. *Ann. Clin. Lab Sci.*, **5**, 348–354.
52. Peters, A., Palay, S.L. and Webster, H.D. (1976) The Fine Structure of the Nervous System, Saunders Company, Philadelphia.